The Seckel syndrome and centrosomal protein Ninein localizes asymmetrically to stem cell centrosomes but is not required for normal development, behavior, or DNA damage response in *Drosophila*

Yiming Zheng[a,†], Vito Mennella[b,c,†], Steven Marks[a], Jill Wildonger[d], Esraa Elnagdi[b,c], David Agard[e], and Timothy L. Megraw[a,*]

[a]Department of Biomedical Sciences, Florida State University, Tallahassee, FL 32306-4300; [b]Department of Biochemistry, University of Toronto, Toronto, M5G 0A4, Canada; [c]Cell Biology Program, The Hospital for Sick Children, Toronto, M5G 1X8, Canada; [d]Department of Biochemistry, University of Wisconsin–Madison, Madison, WI 53706; [e]The Howard Hughes Medical Institute and Department of Biochemistry and Biophysics, University of California, San Francisco, San Francisco, CA 94143-2240

ABSTRACT **Ninein (Nin) is a centrosomal protein whose gene is mutated in Seckel syndrome (SCKL, MIM 210600), an inherited recessive disease that results in primordial dwarfism, cognitive deficiencies, and increased sensitivity to genotoxic stress. Nin regulates neural stem cell self-renewal, interkinetic nuclear migration, and microtubule assembly in mammals. Nin is evolutionarily conserved, yet its role in cell division and development has not been investigated in a model organism. Here we characterize the single Nin orthologue in *Drosophila*. *Drosophila* Nin localizes to the periphery of the centrosome but not at centriolar structures as in mammals. However, Nin shares the property of its mammalian orthologue of promoting microtubule assembly. In neural and germline stem cells, Nin localizes asymmetrically to the younger (daughter) centrosome, yet it is not required for the asymmetric division of stem cells. In wing epithelia and muscle, Nin localizes to noncentrosomal microtubule-organizing centers. Surprisingly, loss of *nin* expression from a *nin* mutant does not significantly affect embryonic and brain development, fertility, or locomotor performance of mutant flies or their survival upon exposure to DNA-damaging agents. Although it is not essential, our data suggest that Nin plays a supportive role in centrosomal and extracentrosomal microtubule organization and asymmetric stem cell division.**

Monitoring Editor
Yukiko Yamashita
University of Michigan

Received: Sep 16, 2015
Revised: Mar 18, 2016
Accepted: Mar 28, 2016

This article was published online ahead of print in MBoC in Press (http://www.molbiolcell.org/cgi/doi/10.1091/mbc.E15-09-0655) on April 6, 2016.

†These authors contributed equally to this work.

The authors declare no competing interests.

*Address correspondence to: Tim Megraw (Timothy.megraw@med.fsu.edu).

Abbreviations used: Cnn, centrosomin; GSC, germline stem cell; Mira, Miranda; MTOC, microtubule-organizing center; NB, neuroblast; Nin, Ninein; PCM, pericentriolar material.

INTRODUCTION

Microcephalic primordial dwarfism (PD) is a spectrum of inherited recessive developmental disorders that cause fetal growth failure resulting in severe dwarfism, microcephaly, and cognitive deficiencies (Majewski and Goecke, 1982; Klingseisen and Jackson, 2011; Megraw *et al*., 2011; Chavali *et al*., 2014). The most prevalent PD disorders include Seckel syndrome, microcephalic osteodysplastic PD (MOPD) types I and II, and Meier–Gorlin syndrome. Mutations of at least 14 genes have been associated with PD disorders (Chavali *et al*., 2014). The genes identified for Seckel syndrome encode proteins that are fundamental to centrosome function (NIN, CEP63, CENPJ/CPAP/SAS-4, and CEP152; Al-Dosari *et al*., 2010;

Kalay *et al.*, 2011; Sir *et al.*, 2011; Dauber *et al.*, 2012) and the DNA damage response (ATR, ATR-interacting protein [ATRIP], DNA2, and RBBP8/CTIP; O'Driscoll *et al.*, 2003; Qvist *et al.*, 2011; Ogi *et al.*, 2012; Shaheen *et al.*, 2014). However, whether the functions of all of these genes are integrated into a common pathway responsible for Seckel syndrome is unclear (Arquint *et al.*, 2014; Chavali *et al.*, 2014; Antonczak *et al.*, 2016).

The centrosome is the major microtubule-organizing center (MTOC) in most animal cells. It is composed of a pair of centrioles (a mother and its daughter), which organize a supramolecular protein assembly (Mennella *et al.*, 2014; Woodruff *et al.*, 2014), the pericentriolar material (PCM), where microtubule assembly and anchoring is regulated. During late mitosis, the pair of centrioles inherited by each cell mature, allowing them to assemble PCM and become centrosomes. Then, after centriole duplication in S phase, only the mother centriole is largely responsible for organizing the PCM at mitotic centrosomes (Wang *et al.*, 2011). Although the centrosome is dispensable for proper cell division (Megraw *et al.*, 1999; Khodjakov *et al.*, 2000; Lecland *et al.*, 2013) and even for most of *Drosophila* development (Megraw *et al.*, 2001; Basto *et al.*, 2006; Debec *et al.*, 2010), mutations in the core centrosome machinery result in a spectrum of diseases that cause primordial dwarfisms and impairment of brain development (microcephaly; Megraw *et al.*, 2011; Chavali *et al.*, 2015). *NIN* was recently identified as one of the genes that cause Seckel syndrome when mutated (Dauber *et al.*, 2012). However, despite its importance to human health and mammalian brain development, the functions of Ninein (Nin) at the developmental, cellular, and molecular levels are not clearly defined.

In mammals, Nin is enriched around the centriole wall and at the subdistal appendages, structures present only on the mother centriole (Ou *et al.*, 2002), which can anchor microtubules to the centrosome (Delgehyr *et al.*, 2005). Nin and its paralogue in vertebrates, Ninein-like protein (Nlp), are γ-tubulin complex–associated proteins that regulate microtubule nucleation and anchoring at centrosomes and noncentrosomal MTOCs (Mogensen *et al.*, 2000; Casenghi *et al.*, 2003; Delgehyr *et al.*, 2005).

In mouse embryonic neural progenitor cells, the older (mother) centrosome is inherited by the self-renewing stem cells at each asymmetric division (Wang *et al.*, 2009). RNA interference (RNAi)–mediated Nin knockdown in embryonic mouse brains in utero disrupted asymmetric segregation of mother and daughter centrosomes and also reduced the number of radial glia progenitors in the developing neocortex of mice, indicating that Nin was required for maintaining asymmetric centrosome inheritance and suggesting that this regulates progenitor self-renewal (Wang *et al.*, 2009). In zebrafish, knockdown of *nin* expression with morpholinos impairs growth and development of the midbrain-hindbrain boundary and formation of the anterior neuroectoderm (Dauber *et al.*, 2012). Despite these loss-of-function studies on mammalian Nin using RNAi and morpholino approaches, there have been no mutant studies of Nin, and no whole-organism disease model has been established to study Seckel syndrome caused by disruption of Nin.

Here we identify the protein encoded by the *Blastoderm-specific gene 25D* (*Bsg25D*, hereafter referred to as *ninein* or *nin*) as the apparent sole homologue of the Ninein family in *Drosophila*. We present genetic, cell biological, and biochemical evidence that Nin shares key similarities with its mammalian counterpart but also some striking differences.

RESULTS

A single Nin-family orthologue in *Drosophila*

To identify putative members of the Nin family in *Drosophila,* we performed a sequence alignment search using the National Center for Biotechnology Information PSI-BLAST program with the N-terminal region of human Nin as a query. This portion of Nin protein sequence contains two regions conserved in the Nin family in mammals, and it was shown to associate with components of the γTurc complex by immunoprecipitation (Casenghi *et al.*, 2003; Delgehyr *et al.*, 2005). In contrast to the rest of the Ninein primary sequence, the N-terminal domain is also not predicted to be coiled-coil and is therefore more likely to be conserved throughout evolution. This analysis identified the gene *Bsg25D* (*CG14025*) as the putative member of the *ninein* family in *Drosophila* (Figure 1). Subsequent phylogenetic analysis revealed that lower metazoan species possess a single *nin* ancestor gene that might have duplicated in the phylum Chordata. In addition to the apparent homology ascertained from sequence similarity, we also found Nin associated with other centrosome proteins (Gopalakrishnan *et al.*, 2011).

Nin can assemble microtubule-organizing centers

To test whether *Drosophila* Nin shares the microtubule anchoring and nucleation function of vertebrate Nin, we expressed Nin–green fluorescent protein (GFP) in S2 cells, a *Drosophila* cell line of embryonic origin. For this and all experiments in which a *nin* transgene was expressed, the protein encoded by the *nin*-RB isoform was used (see Figure 6A later in this paper and *Materials and Methods*). In the majority of S2 cells, Nin accumulated in large cytoplasmic assemblies and occasionally clustered in the proximity of the plasma membrane. The Nin-GFP foci in S2 cells were sufficient to establish a partial reorganization of the microtubule cytoskeleton into a polarized microtubule array (Figure 2A and Supplemental Figure S1A). This is remarkable, considering that in interphase S2 cells, centrosomes normally do not act as major microtubule-organizing centers and microtubules are nucleated from many regions in the cytoplasm, including Golgi membrane (Rogers *et al.*, 2008). Nin structures were not associated with Golgi markers, as shown by costaining with dGMAP, and do not appear to induce Golgi dispersal, in contrast to mammalian cells (Casenghi *et al.*, 2005; Figure 2A). Nin colocalized partially with centrosomin (Cnn), a component of the PCM, but was more concentrated in the space surrounding the PCM (Figure 3, B and C).

To better understand the mechanism of microtubule organization by Nin, we observed individual microtubule nucleation events by labeling the plus end of growing microtubules with the plus end–tracking protein EB1 in S2 cells expressing Nin-GFP (Figure 2, B and C). Live-cell imaging experiments show an enrichment of plus ends of growing microtubules in the region where Nin is concentrated and apparent microtubule anchoring (Supplemental Videos S1–S4). Pairwise distance analysis of the points of emergence of EB1 comets shows that in the presence of Nin, microtubule nucleation sites cluster together when compared with wild-type cells expressing EB1–monomeric red fluorescent protein (mRFP alone), which normally grow microtubules from many regions in the cytoplasm. The N-terminal conserved domain associates with γ-tubulin in *Drosophila* (Figure 2D), consistent with the ability of mammalian Nin to bind γ-tubulin complex components (Casenghi *et al.*, 2003; Delgehyr *et al.*, 2005). However, sites of microtubule clustering established by Nin overexpression in S2 cells are not enriched in γ–tubulin (unpublished data). Taken together, these experiments demonstrate that *Drosophila* Nin has the capacity to function similarly to vertebrate Nin as a regulator of microtubules at centrosomes.

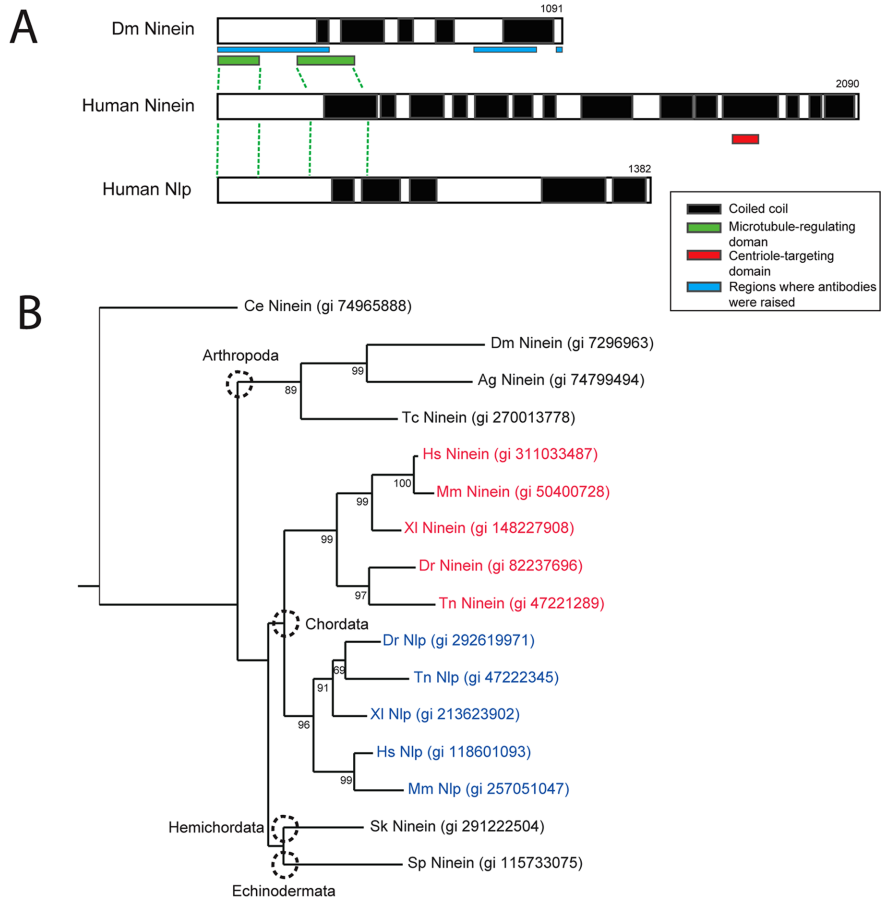

FIGURE 1: *Drosophila* Nin (*Bsg25D* or *CG14025*) is the sole ortholog of mammalian Ninein and Ninein-like protein (Nlp). (A) The Ninein (Nin) family members share a highly conserved domain near the N-terminus that regulates microtubule assembly (shown as a green box), and multiple coiled-coil regions. Mammalian Nin has a centriole-targeting domain (red box) that is not conserved in *Drosophila* or in the mammalian paralog. The sequences corresponding to polypeptides used to raise antibodies are indicated. (B) Tree showing phylogenetic relationships among the Nin orthologues and paralogs. (C) Results of BLAST alignments show that Drosophila Nin has significant similarity to human Nin and Ninein-like protein (Nlp). Protein sequences conserved among Nin orthologues of metazoans are highlighted in red, and those conserved among Nlp orthologues are highlighted in blue. Note that *Drosophila* Nin shares residues with both Nin and Nlp (highlighted in green).

Nin is localized at the periphery of centrosomes and to noncentrosomal MTOCs

To examine the endogenous localization of *Drosophila* Nin, we generated and acquired antibodies that recognize different regions of Nin (Figure 1A) and used the antibodies to examine Nin localization in early cleavage-stage embryos. We selected this tissue because during early embryogenesis, centrosomes organize microtubules throughout the cell cycle, and previous studies suggested that Nin is highly expressed at this stage of development (Boyer *et al.*, 1987). Antibody staining revealed that Nin localizes to the vicinity of centrosomes in blastoderm embryos and is enriched in pole cells, the precursor of germline cells (Figure 3, A and B), where it remains highly expressed in primordial germ cells late into embryogenesis (Supplemental Figure S2). We found that Nin localizes to the periphery of the centrosome, with only a partial overlap with the pericentriolar region labeled with antibodies against Cnn (Figure 3B). The Nin signal is higher at interphase centrosomes than at mitotic centrosomes (Figure 3B; see also Supplemental Figure S3), similar to the cell cycle dynamics reported for Nin in mammals (Mogensen *et al.*, 2000; Casenghi *et al.*, 2003). In addition to Nin localization by antibody staining, we constructed Nin-myc and Nin-GFP transgenic flies and examined their localization and dynamics in fixed and live embryos. The localization of Nin-myc was similar to endogenous, except that a higher signal could be seen at mitotic centrosomes (Figure 3C), likely because of overexpression. Live imaging by spinning-disk confocal microscopy of *Drosophila* early embryos expressing Nin-GFP shows that Nin is dynamically distributed at the centrosome periphery during the cell cycle, with enrichment at interphase centrosomes (Supplemental Figure S3 and Supplemental Videos S5 and S6). The localization and dynamics of Nin-GFP in live embryos are consistent with the distribution of endogenous Nin observed by antibody staining on fixed *Drosophila* embryos (Figure 3B).

Mammalian Nin was shown to localize to noncentrosomal MTOCs in specialized cell types (Mogensen *et al.*, 2000). In *Drosophila* wing epithelial cells and myocytes, which organize microtubules from MTOCs at adherens junctions near the apical membrane and at perinuclear sites, respectively (Tassin *et al.*, 1985; Mogensen *et al.*, 1989; Bugnard *et al.*, 2005), Nin was localized to these MTOCs (Figure 4). In wing epithelial cells, where previous reports showed that microtubules

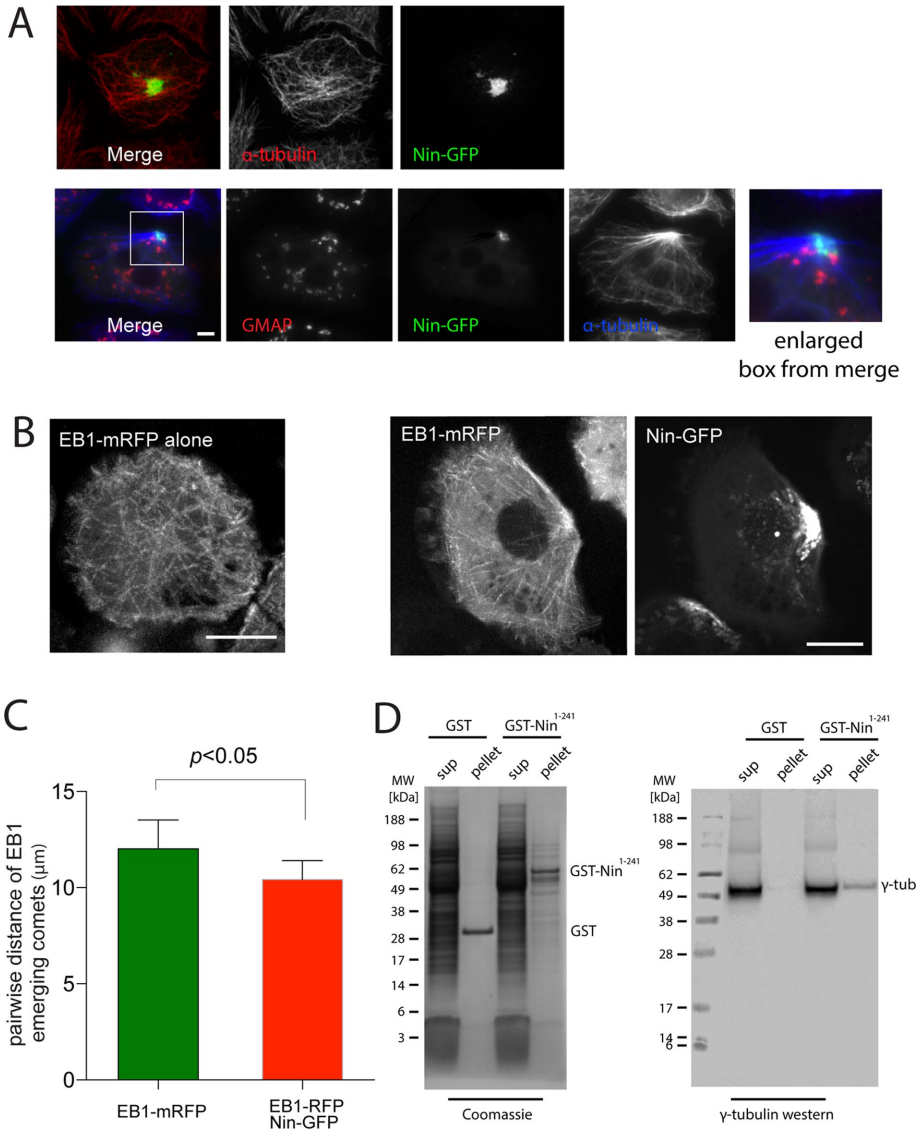

FIGURE 2: Nin organizes microtubule-nucleating centers when overexpressed in *Drosophila* S2 cells. (A) Images of S2 cells expressing Nin-GFP. Microtubules are labeled with antibodies against α-tubulin, and Golgi with antibodies against GMAP. See also Supplemental Figure S1A. Scale bar, 5 μm. (B) Images of EB1-mRFP microtubule plus-end tracks in S2 cells with expression of Nin-GFP (bottom) or without (top). See also Supplemental Videos S1–S4. (C) Pairwise distance of EB1 emerging comets. Pattern of MT nucleation sites measured by plotting the point of emergence of each EB1 particle and correlating it with emergence of its neighbors. (D) GST-Nin N-terminal 241 amino acid domain binds to γ-tubulin in S2 cell lysates.

organized from the adherens junctions near the apical membrane (Matis *et al.*, 2014), we found that Nin was localized to a focus at the center of this MTOC (Figure 4C) and was not localized at centrosomes (Figure 4, A and B). This pattern was the same in wing disks from early third-instar larvae (unpublished data) or wandering stages (Figure 4). In muscle from third-instar larvae, Nin localized to the perinuclear MTOCs (Figure 4D). Thus Nin localizes to noncentrosomal MTOCs in *Drosophila*.

Nin localizes with an asymmetric bias to daughter centrosomes when overexpressed in stem cells

Given the requirement of Nin for the asymmetric segregation of centrosomes in mouse embryonic neural progenitor cells (Wang *et al.*, 2009), we investigated the Nin localization pattern in *Drosophila* stem cells. In *Drosophila* germline stem cells (GSCs) and neuroblasts (NBs), the centrosomes are segregated asymmetrically during cell division (Rusan and Peifer, 2007; Yamashita *et al.*, 2007; Januschke *et al.*, 2011, 2013). In male GSCs, the older, "mother" centrosome is retained in the GSC at each self-renewal, with the centrosome anchored at the apical membrane adjacent to the "hub," the niche where the GSC resides (Yamashita *et al.*, 2007). In the ovary, this asymmetry is inverted, and the younger, daughter centrosome is retained in the GSC (Salzmann *et al.*, 2014). In NBs, the younger, daughter centrosome is retained in the self-renewed stem cell and retains PCM and MTOC activity in interphase, whereas the mother centrosome becomes inactivated until mitosis. This segregation pattern in NBs is opposite to what occurs in mouse neural progenitors, where the mother centrosome is retained by the self-renewed progenitors (Rusan and Peifer, 2007; Wang *et al.*, 2009; Conduit and Raff, 2010; Januschke *et al.*, 2011, 2013).

In larval brain NBs, we were unable to detect endogenous Nin localization to centrosomes with anti-Nin antibodies (unpublished data). However, in larval brain NBs expressing either Nin-myc (Figure 5A) or Nin-GFP (Supplemental Figure S1, B and C), Nin exhibited pericentrosomal localization, as revealed by largely nonoverlapping localization in close proximity to Cnn, similar to the pattern in embryos (Figure 3, B and C). Using Cnn to differentiate mother and daughter centrosomes, as Cnn is enriched at the daughter centrosome in NBs (Rusan and Peifer, 2007; Conduit and Raff, 2010; Januschke *et al.*, 2011), we found that Nin preferentially accumulated at the younger, daughter centrosome rather than with the older, mother centrosome in NBs (Figure 5A). Nin localization at the daughter centrosome is cell cycle regulated in NBs, as Nin expression was only detected in interphase or early mitotic NBs and became undetectable at centrosomes by metaphase of mitosis. In male GSCs, expression of Nin-myc revealed that Nin localization was enriched preferentially at the daughter centrosome in this stem cell population too (Figure 5B). In contrast with Nin asymmetric localization in GSCs and NBs, Nin is symmetrically localized to centrosome pairs in embryos (Figure 3B) and ganglion mother cells in the developing brain (Supplemental Figure S1C), consistent with their symmetrical cell division characteristics.

Despite the provocative asymmetric localization observed with Nin transgene expression in NBs, we failed to detect endogenous Nin expression at larval NB centrosomes by immunofluorescence staining despite detection of Nin in lysates of whole brains by Western blotting (see later discussion). Whether this result reflects a lack of endogenous Nin expression in larval brain NBs or is due to insufficient sensitivity of our Nin antibodies is unclear. However, to

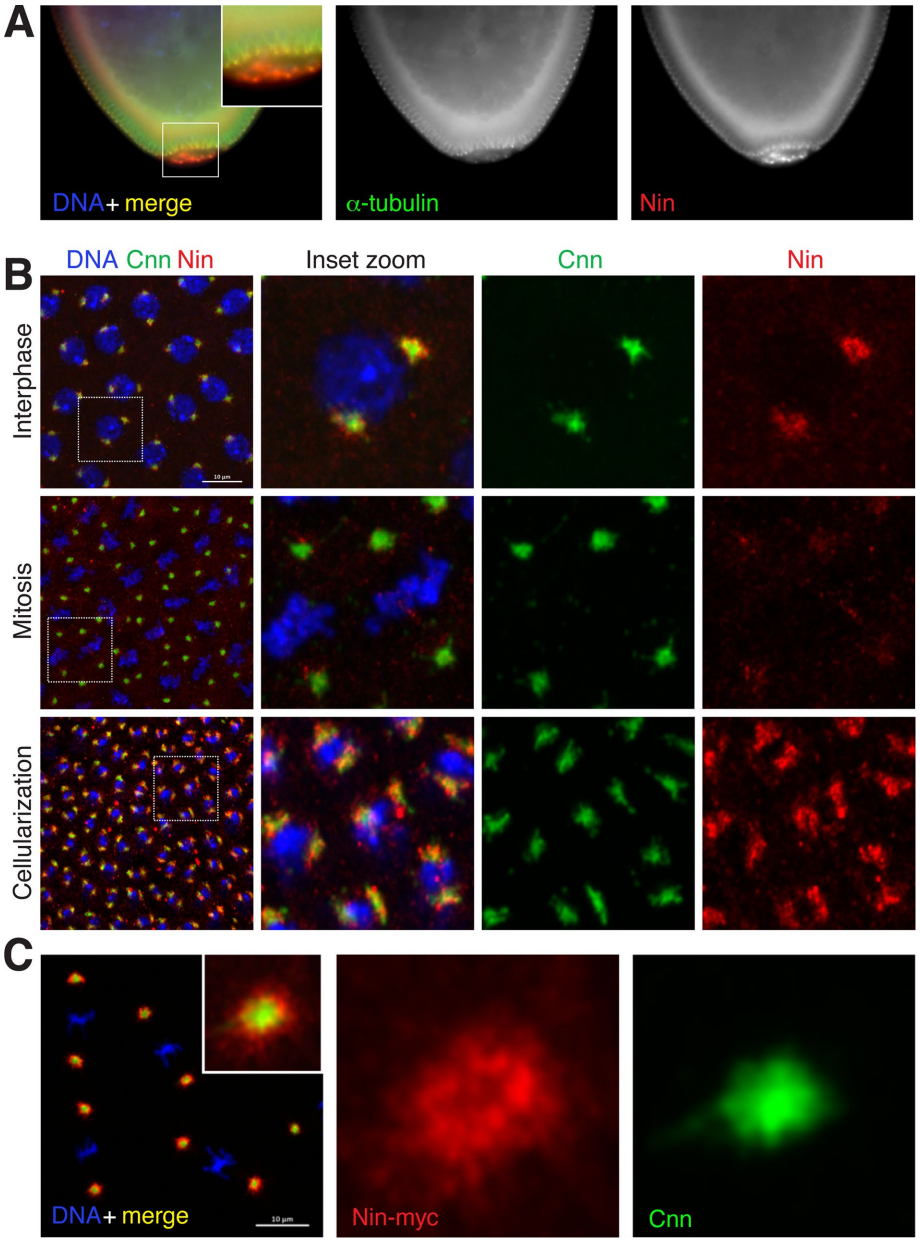

FIGURE 3: Nin is a pericentrosomal protein. (A) Relatively higher expression of endogenous Nin in the germline precursor (pole) cells in early embryos. Fixed wild-type embryos were stained with the C-terminal Nin antibody. See also Supplemental Figure S2. (B) Pericentrosomal localization of endogenous Nin in cleavage stage embryos. Shown are cycle 12–13 embryos and stage 14 (cellularization) stained with antibodies to the N-terminal region of Nin. Nin signal is highest in interphase, and relatively reduced in mitosis. (C) Pericentrosomal localization of Nin-myc in embryos. Fixed embryos expressing Nin-myc were stained with anti-myc for Nin expression (red), anti-Cnn for centrosome PCM (white) and 4′,6-diamidino-2-phenylindole (DAPI) for DNA (blue). Scale bar, 10 μm

examine a role for Nin in NB division and polarity, we generated a *nin* mutant allele and tested its function in NB asymmetric division.

nin^{1} is a deletion allele that disrupts *nin* expression

To study the functions of Nin, we sought a mutant allele of the *nin* gene by mobilizing a P element transposon located within the 5′ untranslated region of the first exon of the *nin* gene locus (Figure 6A). From the P element excision, we isolated one allele that deleted ~3.5 kb of *nin* on the 3′ side of the P element, generating an allele that we designated *nin*^{1}, and which is predicted to disrupt all of the *nin* transcripts (Figure 6, A and B, and Supplemental Figure S4). Because the start codons and a significant portion of the N-terminal coding regions of all *nin* isoforms are deleted, including the N-terminal MT-regulating domain (Figure 1A), *nin*^{1} appears to be a strong allele and likely a null.

To determine whether *nin*^{1} disrupts expression of Nin, we examined Nin protein by Western blot and Nin localization to centrosomes by immunofluorescence analysis (Figure 6, C and D). Whereas endogenous Nin was detected in embryos and larval brain lysates by Western blotting (Figure 6C) using antibodies raised against the N- or C-terminal regions of Nin (Figure 1A), Nin expression was absent in *nin*^{1} embryos and larval brains (Figure 6, C and D).

Nin is not essential for neuroblast asymmetric division and self-renewal or for adult locomotor performance

Although mutation of human *NIN* disrupts normal development, resulting in Seckel syndrome (Dauber *et al.*, 2012), surprisingly, *nin*^{1} mutant flies are homozygous viable, appear to develop normally, are fertile, and have no overt morphological or behavioral phenotypes. Because *nin* knockdown by RNAi in mice showed that Nin is essential for embryonic neural progenitor asymmetric division and self-renewal (Wang *et al.*, 2009), we investigated these functions in *nin*^{1} mutant flies. In contrast with its role in mice, we found that *nin*^{1} NBs did not lose asymmetric division characteristics during mitosis (Figure 7, A and B), as revealed by normal localization of the NB marker and basal polarity protein Miranda (Mira; Cabernard and Doe, 2009) and apparently normal centrosome asymmetry with regard to Cnn localization during the NB cell cycle. Moreover, spindle orientation with respect to NB polarity, which is disrupted in some centrosome protein mutants (Giansanti *et al.*, 2001; Megraw *et al.*, 2001; Singh *et al.*, 2014), was normal (Figure 7B). Accordingly, there was no significant change in the number of Mira-positive NBs between wild-type and *nin*^{1} mutant larval central brains (Figure 7C and Supplemental Figure S5), indicating that *Drosophila* Nin, in contrast to mammalian Nin, is not essential for NB asymmetric division and self-renewal. We did not assess *nin*^{1} GSCs for proper asymmetric division.

Proper NB proliferation is essential to generate sufficient neurons to populate the nervous system. A properly functioning nervous system is essential for many neurological activities, including locomotor function. Moreover, Nin is required for cilium assembly in mammalian cells (Graser *et al.*, 2007), and cilia are required for normal locomotor function in *Drosophila* (Eberl *et al.*, 2000; Caldwell *et al.*, 2003). Therefore we evaluated the locomotor performance of *nin*^{1} adult flies using a climbing assay and determined that *nin*^{1}

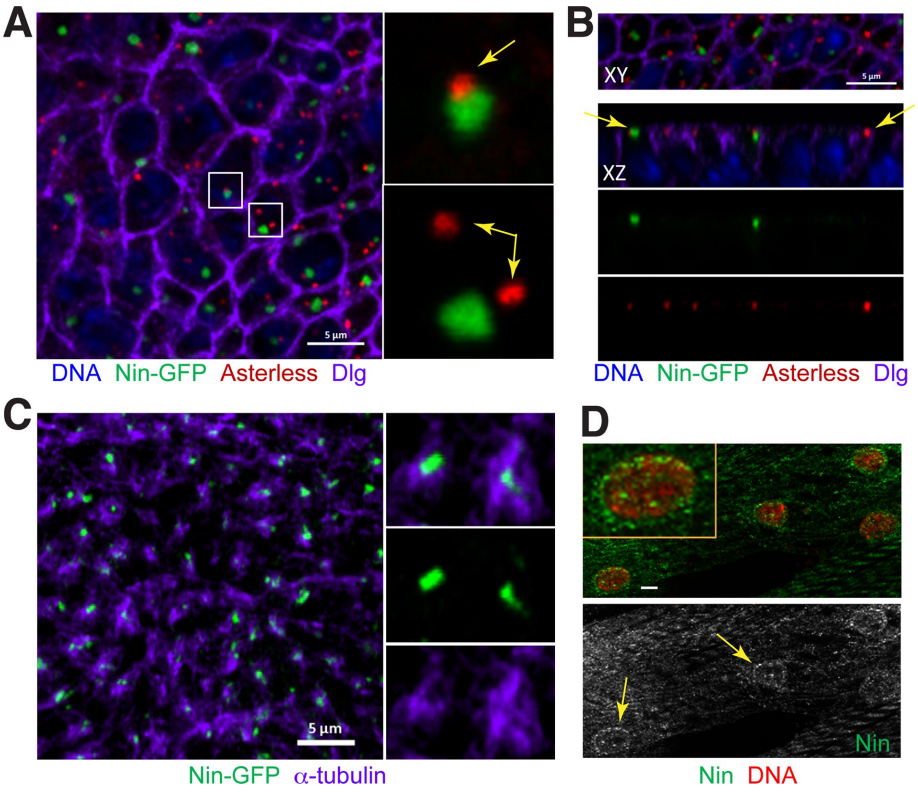

FIGURE 4: Nin localizes to noncentrosomal MTOCs in wing epithelia and myocytes. (A) Nin-GFP associates with the noncentrosomal MTOC in wing epithelia. In the columnar epithelial cells of the developing wing disk, Nin-GFP (green) localizes primarily to one focus in each cell. The focus of Nin-GFP colocalizes adjacent to centrosomes ~20% (29/156) of the time (top inset), and is unassociated in ~80% (127/156) of cells (yellow arrows in insets). Centrosomes labeled with antibodies against asterless (asl), red). Dlg (purple) is an apical membrane marker. Image is an *xy* view of a third instar larval wing pouch epithelium z-stack projection. (B) Images of Nin-GFP foci in *xy* and *xz* views of the wing disk. These views demonstrate that Nin-GFP foci and centrosomes are both localized near the apical membrane in wing epithelia (yellow arrows). (C) Nin-GFP (green) localizes to the center of the noncentrosomal MTOCs labeled with α-tubulin (purple). (D) Myocytes in third instar larval muscles stained for endogenous Nin (green) using the C-terminal Nin antibody and DAPI (red) show that Nin has perinuclear localization. Yellow arrows point to the Nin localization at the periphery of myocyte nuclei. Scale bars: 5 µm in A–C, 1 µm in D.

mutant flies behaved similarly to wild type (Figure 7D), suggesting that Nin is not essential for normal nervous system development or function.

Nin is not essential for embryo development

We examined the role of Nin in early embryo development, in which centrosome function is essential for the early cleavage cycles (de Saint Phalle and Sullivan, 1998; Rothwell *et al.*, 1998; Megraw *et al.*, 1999; Vaizel-Ohayon and Schejter, 1999; Kao and Megraw, 2009). In wild-type embryos, Nin is localized to the periphery of centrosomes but absent in nin^{1} mutant embryos (Figure 6D). Nin appears to be dispensable for embryo development, as nin^{1} mutant embryos had only a slightly reduced hatch rate compared with isogenic wild-type (w^{1118}) embryos (84.5 ± 1.0% vs. 87.8 ± 1.1%), an insignificant difference ($p = 0.092$; Figure 8A). Moreover, cleavage furrows and other aspects of cleavage such as spindle morphology and nuclear positioning appeared normal in nin^{1} mutant embryos (Figure 8B and unpublished data), establishing that loss of function of Nin does not overtly affect *Drosophila* embryo development.

Recent reports indicated that Nin associates with Rab11, a small G protein and regulator of endosomal vesicle trafficking (Guruharsha *et al.*, 2011). This is consistent with the pericentrosomal localization of Nin, a pattern similar to that of Rab11, which localizes to vesicles at the periphery of centrosomes during early embryo development (Riggs *et al.*, 2003). Because Rab11 was the only binding partner of Nin recovered in a mass spectrometry screen (Guruharsha *et al.*, 2011), we sought to determine whether Nin and Rab11 have a genetic interaction. To this end, we examined the embryo hatch rate of nin^{1} $Rab11$ double mutants. $Rab11^{93Bi}$ is a hypomorphic allele; homozygotes are viable, and females have reduced fertility due to maternal effect lethality. Double mutants with a combination of nin^{1} and $Rab11^{93Bi}$ are also homozygous viable with reduced female fertility. The nin^{1} mutant decreased the hatch rate of $Rab11^{93Bi}$ embryos from 66.9 ± 2.9 to 58.5 ± 0.5% (Figure 8A). The significance of this enhancement of *Rab11* maternal effect lethality by *nin* is of low significance, however, with *p* close to 0.05. The mild genetic effect could be an additive effect rather than a significant genetic interaction between nin^{1} and $Rab11^{93Bi}$ alleles. Rab11-deficient embryos from transheterozygotes bearing a combination of the amorphic $Rab11^{J2D1}$ allele and $Rab11^{93Bi}$ showed a hatch rate of 8.5 ± 2.0%, consistent with previously published measurements (Jankovics *et al.*, 2001), and combining it with the nin^{1} homozygous mutation lowered the embryo hatch rate to 1.2 ± 1.0% ($p = 0.029$). This decrease in $Rab11^{J2D1}/Rab11^{93Bi}$ embryo survival due to nin^{1} may again be an additive effect rather than a synergistic genetic interaction. Costaining of embryos for Nin and Nuf, a partner of Rab11 that localizes to endosomes, showed that Nin mostly did not colocalize with Nuf (Supplemental Figure S6). We examined Nuf localization in nin^{1} embryos and found no disruption of its pattern of localization (Supplemental Figure S6). We therefore conclude that Nin is not a component of endosomes.

We also evaluated Nin genetic interaction with two centrosome components—Cnn, a PCM protein, and Bld10, a centriolar protein. Mutations in *bld10* are viable, yet mutant males are infertile, whereas females are fertile (Mottier-Pavie and Megraw, 2009; Carvalho-Santos *et al.*, 2012; Roque *et al.*, 2012), whereas *cnn* mutants are maternal effect lethal and male sterile (Li *et al.*, 1998; Megraw *et al.*, 1999; Vaizel-Ohayon and Schejter, 1999). Double mutants of nin^{1} with cnn^{25cn1} or cnn^{hk21} (both are *cnn* null alleles) did not overtly modify phenotypes of *cnn* alone, as observed by adult morphological features and viability. Similarly, double mutants with nin^{1} and $bld10^{c04199}$ or $bld10^{f01951}$ did not modify phenotypes of *bld10* alone, as assessed by adult morphology, viability, and female fertility. Together, these results indicate that Nin does not interact genetically with some centrosome proteins.

Loss of function of Nin does not affect DNA damage response

Because mammalian Nin is implicated in Seckel syndrome (Dauber *et al.*, 2012), we sought to determine whether the nin^{1} mutant has

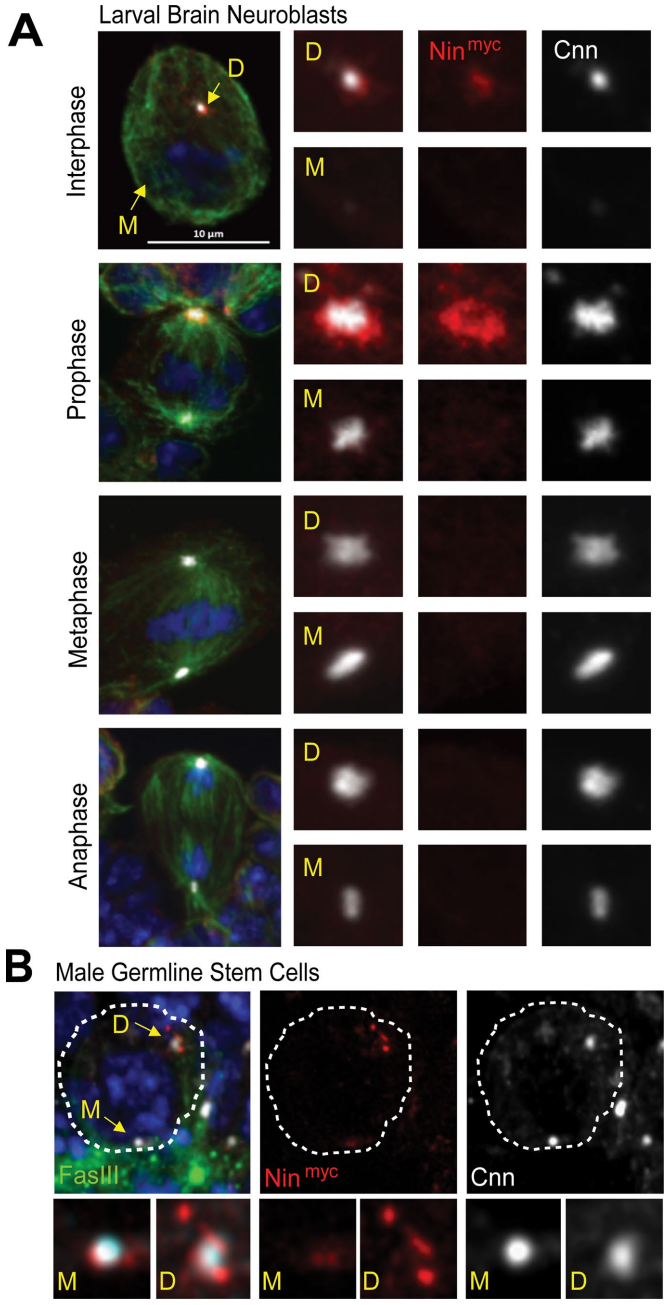

FIGURE 5: Nin localizes asymmetrically to daughter centrosomes in stem cells. (A) Nin-myc localization is asymmetric and enriched at daughter centrosomes in larval brain neuroblasts. Larval brain neuroblasts expressing Nin-myc were stained with anti-myc (red) to reveal Nin expression and localization. Cnn (white) labels centrosomes and their asymmetry (Cnn is enriched at daughter centrosomes), α-tubulin (green) for microtubules (MT), DAPI (blue) for DNA. See also Supplemental Figure S1B, C. M = mother centrosome, D = daughter centrosome. Scale bar, 10 µm. (B) Nin-myc localization at mother and daughter centrosomes in male germline stem cells (GSCs). Male GSCs expressing Nin-myc were stained with anti-myc for Nin expression, anti-FasIII to label the stem cell niche, anti-Cnn for centrosome PCM, and DAPI for DNA.

other pathological features that are associated with Seckel syndrome. One established characteristic of Seckel syndrome is a defective DNA damage response, as exemplified by the ATR mutant (O'Driscoll *et al.*, 2003). Mutants of the *Drosophila* ATR orthologue, *Mei-41*, are similarly sensitive to mutagenic agents like hydroxyurea (HU) or methyl methanesulfonate (MMS). Using a mutation in *mei-41* (*mei-41^{D5}*) as a positive control and *w^{1118}* as a negative control, we found that, like *w^{1118}*, *nin^{1}* mutant flies develop and survive similar to wild type when exposed to 80 µM HU or 0.1% MMS (unpublished data), both of which were lethal to the *mei-41^{D5}* mutant, as shown previously (Banga *et al.*, 1986). Therefore the *nin^{1}* mutant appears to have a normal DNA damage response.

Global overexpression of Nin is lethal

To evaluate the phenotype of Nin gain of function, we overexpressed Nin ubiquitously or in restricted tissues in *Drosophila* and compared it to the overexpression of other centrosomal proteins (Cnn, Bld10, Sas6, and Rab11). Ubiquitous overexpression of Nin-GFP in transgenic flies using Act-Gal4 and Tub-Gal4 drivers resulted in death during the early pupal stage, whereas flies that overexpressed Cnn, Bld10, Sas6, or Rab11 developed normally (Table 1). However, flies developed efficiently and were healthy when Nin was overexpressed only in NBs or throughout the entire nervous system using worniu-Gal4 or Elav-Gal4, respectively. These data indicate that some tissues or cells, but not those of the nervous system, are sensitive to Nin overexpression.

DISCUSSION

In this study, we identify and characterize the function and requirement of the sole member of the Ninein family in *Drosophila* from the cellular to the organismal level. The findings presented here highlight both the conserved roles and the key differences of Ninein in *Drosophila melanogaster* compared with mammalian species in which the majority of the previous studies have been conducted. We found that the disruption of *nin* does not overtly affect cell division, development, viability, fertility, or locomotor behavior in *Drosophila*. These results are surprising, given the conservation of Nin in eukaryotic evolution and its importance in vertebrates revealed by RNAi and morpholino studies. There is no apparent paralogue in flies to account for lack of phenotype, as phylogenetic analysis shows that, wheres many metazoans have two Nin-family paralogues (Ninein and Nlp), *Drosophila* possesses only one orthologue of Nin. However, a recent study in *Caenorhabditis elegans* showed that the ninein orthologue (NOCA-1) functions redundantly with Patronin (Wang *et al.*, 2015), another MT minus end protein, raising the possibility that *Drosophila* Nin might also function in parallel with Patronin (Goodwin and Vale, 2010).

In vertebrates, Ninein is a component of the mother centriole and is enriched in subdistal appendages (Mogensen *et al.*, 2000; Delgehyr *et al.*, 2005), structures required for microtubule anchoring and ciliogenesis. In further contrast to vertebrate Nin, we find that *Drosophila* Nin localizes to the periphery of the centrosome and does not reside at centrioles. This difference in localization might be explained at least in part by the absence of mother centriole appendage structures in *Drosophila* centrioles. In addition, *Drosophila* Nin appears to lack the centriole-targeting domain found in vertebrate Nin (Figure 1A). The higher accumulation of Nin at interphase versus mitotic centrosomes in embryos correlates directly with the relative intensity of astral microtubules at embryonic cleavage-stage centrosomes, which are higher in interphase and lower in metaphase (Karr and Alberts, 1986), suggesting that Nin localization might depend on MTOC activity or may localize to MT minus ends together with Patronin, as recently shown in *C. elegans* (Wang *et al.*, 2015).

Despite the differences in centrosomal localization, one aspect of Nin localization—its asymmetric localization in neural stem cells—suggests conservation of function with vertebrates with regard to

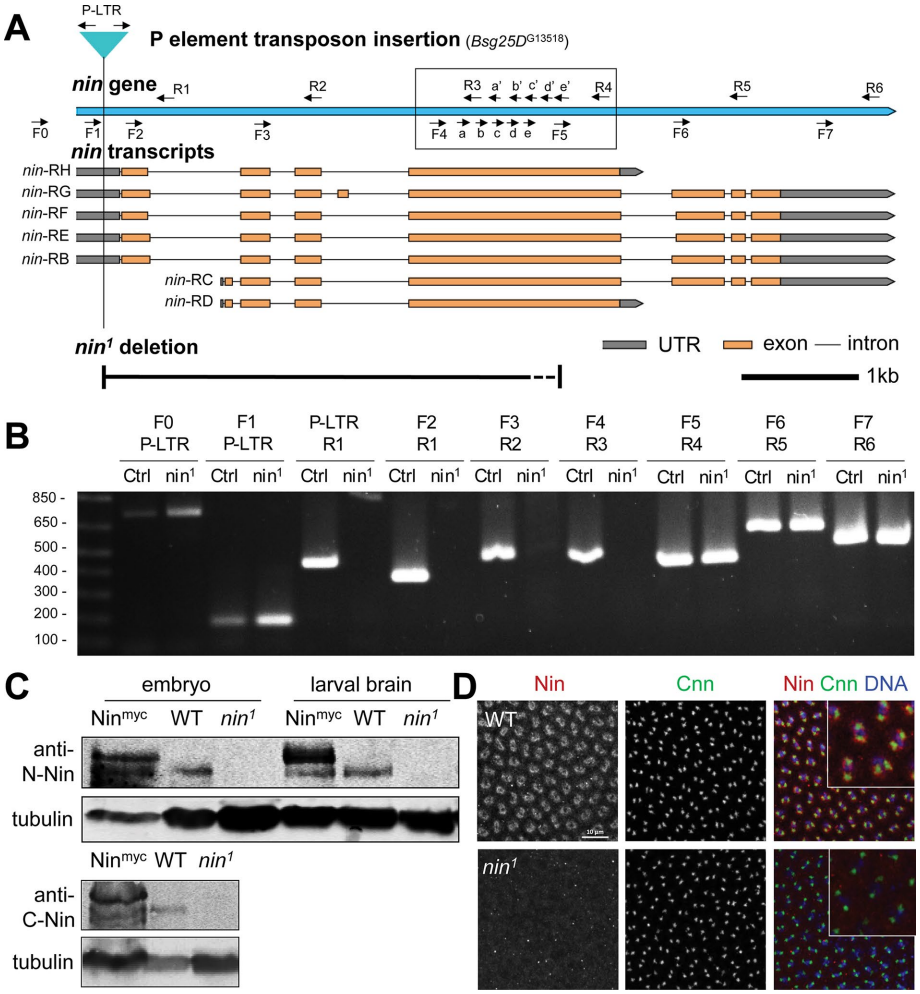

FIGURE 6: *nin*^{1} is a deletion allele that disrupts *nin* expression. (A) Schematic view of *Drosophila nin* locus, transcripts, P element insertion (G13518) and *nin*^{1} deletion. The *nin*^{1} deletion allele was generated by mobilizing the P element transposon, *Bsg25D*^{G13518}, located in the 5′ UTR. The primer pairs used for PCR screening are indicated (arrows). The primer pairs in the boxed region were used to narrow down the region deleted in *nin*^{1}. The dotted line section of the deletion represents the region where the 3′ breakpoint of the *nin*^{1} deletion resides: somewhere between the "e" and "F5" primer sites. The scale bar is 1 kb. (B) Single adult fly PCR analysis of *nin*^{1}, which shows a deletion of ~3.5 kb. The PCR results for the primer pairs in the boxed region are shown in Supplemental Figure S4. Control (Ctrl) represents the original P element insertion stock that was used to generate the *nin*^{1} deletion allele. Sequences for the primers are listed in Supplemental Table S1. (C) Western blot analysis of *nin*^{1} embryo and larval brain lysates using an antibody against the N-terminal region of Nin, and in embryo lysates also using a C-terminal antibody. The Nin-myc transgene shows endogenous and myc-tagged Nin bands with an ~150 kDa M_r, there is 6.4-fold increase in the tagged Nin expression compared with the endogenous Nin. Wild-type shows endogenous Nin bands, which are absent in *nin*^{1} lysates. α-tubulin serves as loading control. (D) Immunofluorescence staining of wild-type and *nin*^{1} embryos. Fixed embryos were stained with antibodies against endogenous Nin N-terminal region, and with Cnn antibody to mark centrosomes. The inset shows magnified view of Nin and Cnn in embryos.

neural stem cell division and self-renewal in *Drosophila*. However, whereas mouse Nin is localized preferentially to the mother centriole, it appears equally distributed between the centrosomes in neural progenitor cells (Wang *et al.*, 2009). *Drosophila* Nin, on the other hand, is localized preferentially to the younger, daughter centrosome and is barely detectable at the older, mother centrosome at the basal side of the NB, even at early mitosis, when PCM accumulates on the mother centrosome. This asymmetric localization of Nin in NBs is also recapitulated in male germline stem cells, where again Nin is enriched at the daughter centrosome and is expressed at relatively higher levels in the primordial germ cells (pole cells). The localization of Nin in both of these stem cells suggests a possible function in asymmetric cell division, which was not revealed upon depletion of Nin by the *nin*^{1} mutant.

The strong *nin* allele that we generated, *nin*^{1}, disrupts *nin* expression. The mutant flies are viable and show no overt phenotypes. After carefully evaluating phenotypes in neural stem cells and embryos, we conclude that *Drosophila* Nin does not play an essential role in the nervous system or in early embryo development. Because human *NIN* is mutated in SCKL syndrome, which results in severe developmental defects and has etiological links to DNA damage response, it is further surprising that requirements for Nin in development and the DNA damage response were not conserved in *Drosophila*. Taken together, our findings indicate that Nin plays a less critical role in flies than in *C. elegans* or vertebrate species.

On the basis of these findings, we speculate that Nin functions differently in *Drosophila* neuroblasts than in mammalian neural progenitors (Wang *et al.*, 2009). Athough no clear *nin* paralogues are present in *Drosophila*, it remains possible that other protein(s) are functionally redundant with Nin, masking any phenotypes in the *nin*^{1} mutant. Therefore, although Nin is not essential for *Drosophila* development, it may well have important functions that were not revealed by these experiments.

MATERIALS AND METHODS

Drosophila stocks

w^{1118} was used as wild-type control. The *nin*^{1} deletion mutant is described later. The following stocks were obtained from the Bloomington *Drosophila* Stock Center with stock numbers indicated or from cited sources: *Bsg25D*^{G13518}/CyO (*nin* P element insertion allele; BL#28091), Df(2L)Exel6011 (BL#7497), *Rab11*^{93Bi}/TM3 (BL#4158), *Rab11*^{J2D1}/TM3 (BL#12148), *cnn*^{25cn1}/CyO, Kr-GAL4^{DC3} UAS-GFP^{DC7}, *cnn*^{hk21}/CyO, Kr-GAL4^{DC3} UAS-GFP^{DC7} (Megraw *et al.*, 1999), *bld10*^{c04199}/TM6B and *bld10*^{f01951}/TM6B (Mottier-Pavie and Megraw, 2009), and *mei-41*^{D5} (BL#4236). Transgenic stocks were UAS-Nin-GFP and UASp-Nin-myc (this study), UASp-GFP-Cnn (Zhang and Megraw, 2007), UASp-Bld10-GFP (Mottier-Pavie and Megraw, 2009), UASp-Sas6-GFP/TM6B (Peel *et al.*, 2007), and UASp-YFP-Rab11/TM3 (BL#9790). Transgenes were expressed ubiquitously by using TubP-Gal4^{LL7} (BL#5138) or Act5C-Gal4^{E1} (BL#25374) in the nervous system using Elav-Gal4^{C155} (BL#458), in the germline using Nanos-Gal4-VP16 (BL#4937), in neuroblasts using Worniu-Gal4 (Singh *et al.*, 2014), and in wing disks using MS1096-Gal4 (BL#25706) or Nubbin-Gal4 (BL#25754). Flies were maintained with standard food at 25°C.

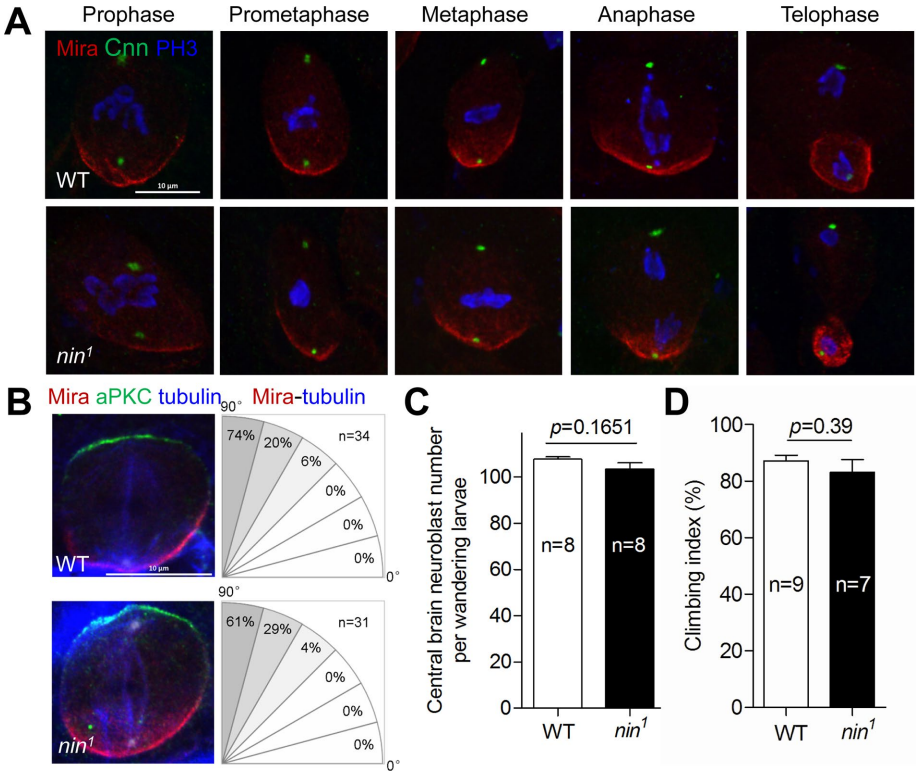

FIGURE 7: Nin is not essential for neuroblast asymmetric division and self-renewal, or for normal locomotor function. (A) Representative images showing the normal asymmetric division of *nin*^{1} larval brain NBs at the indicated stages of the cell cycle. Mira staining (red) is a NB basal marker of cell polarity, phospho-histone 3 (PH3, blue) for mitotic cells, Cnn (green) for centrosome PCM. (B) Polarity and spindle orientation are normal in *nin*^{1} NBs. Left: NBs were stained with anti-Mira (red), anti-aPKC (green) for basal and apical polarity, respectively, and anti-α-tubulin (blue) for microtubules. Right: the percent spindles oriented along the polarity axis, in 15 degree increments, is quantified. (C) Quantification of central brain Mira-positive nuclei shows normal number of NBs in *nin*^{1} larval brains. See Supplemental Figure S6 for representative staining. (D) Climbing (negative geotaxis) assay shows normal locomotor performance for *nin*^{1} adult flies. Error bars in C and D indicate SE of the means (SEM).

Generation of UAS-Nin-GFP and UASp-Nin-myc transgenes

The Nin coding sequence corresponding to the *nin*-RB isoform (Figure 6A) was amplified by PCR from the LD21844 cDNA clone obtained from the *Drosophila* Genetics Resource Center (DGRC). The sequence, including the ATG codon and encompassing the entire open reading frame (ORF) up to the last codon but excluding the stop codon, was amplified by PCR using ninRB-F1 and ninRB-R1 (Supplemental Table S1) and cloned into the pENTR vector (Life Technologies, Carlsbad, CA). The ORF was transferred by the Gateway system (Life Technologies) into several expression vectors (Terence Murphy [Carnegie Institution for Science] and DGRC), which were modified by insertion of the attB sequence: pTWG-attB and pPWM-attB vectors were constructed by cloning a 368–base pair fragment containing the *attB* sequence PCR amplified from pVALIUM1 (base pairs 2567–2935) using primers *attB*-F1 and *attB*-R1 (Supplemental Table S1) into the *Aat*II restriction site of pTWG and pPWM (at the 1989–base pair position in both vectors), respectively (Chen and Megraw, 2014). Transgenic flies were generated by Genetivision. These *nin* transgenes were inserted at a PhiC31 landing site (VK22:(2R)57F5). For the imaging experiments described in Supplemental Figure S3 and Supplemental Videos S5 and S6, the Nin coding sequence corresponding to the *nin*-RB isoform tagged with GFP at its C-terminus was PCR amplified with ninRB-F2 and ninRB-R2 primers (Supplemental Table S1), cloned into pUASp-K10attb construct (a kind gift of B. Suter, Institute of Cell Biology, University of Bern, Bern, Switzerland; Gene Bank EU729723), and recombined into the fly genome at the PhiC31 landing site 51D9.

Phylogenetic analysis

The putative non–coiled-coil region of the Nin-PB isoform (amino acids 1–341) was used as a bait to run three rounds of PSI BLAST. Most genes homologous to Ninein were identified after only one round of PSI BLAST, whereas the *C. elegans* homologue was identified after two rounds, suggesting a high degree of sequence divergence in this species. Every identified gene was then reversed BLASTed against the *Drosophila* genome. No clear homologue of Ninein was found in the yeast model organisms *Saccharomyces cerevisiae* and *Schizosaccharomyces pombe*. After identification of several genes with homology to Nin in different species, the N-terminal 1– to 341–amino acid sequence was used to run a sequence alignment by using the program MAFFT. The phylogenetic tree was built with the neighbor-joining method using *C. elegans* sequence as outgroup; bootstrap analysis was performed using the program MacVector

Immunofluorescence and live-cell imaging of S2 cells

The *nin*-RB ORF was cloned into the pAWG and pMT/V5-HIS expression vectors for expression in *Drosophila* Kc167 cells and S2 cells, respectively. Transfections were performed with Lipofectamine 2000 (Life Technologies) or Effectene (Qiagen, Hilden, Germany). Ectopic expression of fluorescently tagged Nin in S2 cells was driven by addition of $CuSO_4$ at a final concentration of 300 μM. Immunostaining was performed as described (Kao and Megraw, 2004; Mennella *et al.*, 2012). Live-cell imaging on S2 cells and *Drosophila* embryos was performed as previously described (Rogers *et al.*, 2002). Images were acquired with a Zeiss Axiovert 200M equipped with a 100×/1.45 numerical aperture oil objective and an electron-multiplying charged-coupled device camera (C9100-13; Hamamatsu Photonics, Japan). The 488-nm line of an argon laser or the 561-nm line of a krypton laser was used for illumination, attached to a spinning-disk confocal scan head (CSU10; Yokogawa; obtained from Solamere).

Analysis of microtubule dynamics in *Drosophila* cells

Drosophila S2 cells were cotransfected with expression plasmids (pMT/V5His) encoding EB1-GFP or EB1-RFP (Mennella *et al.*, 2005) plus Nin-GFP. At 48 h after transfection, expression was induced by addition of $CuSO_4$. Cells were subsequently plated on #1.5 glass-bottom MatTek dishes for 4 h and imaged by spinning-disk confocal fluorescence microscopy. The pixel coordinates of newly emerging EB1 comets were obtained by analysis of the maximum intensity projections of the recorded time-lapse video. The pairwise distance between each of the individual new EB1 comets in the time lapse was determined with an Excel macro. Statistical analysis was performed with Kaleidagraph software.

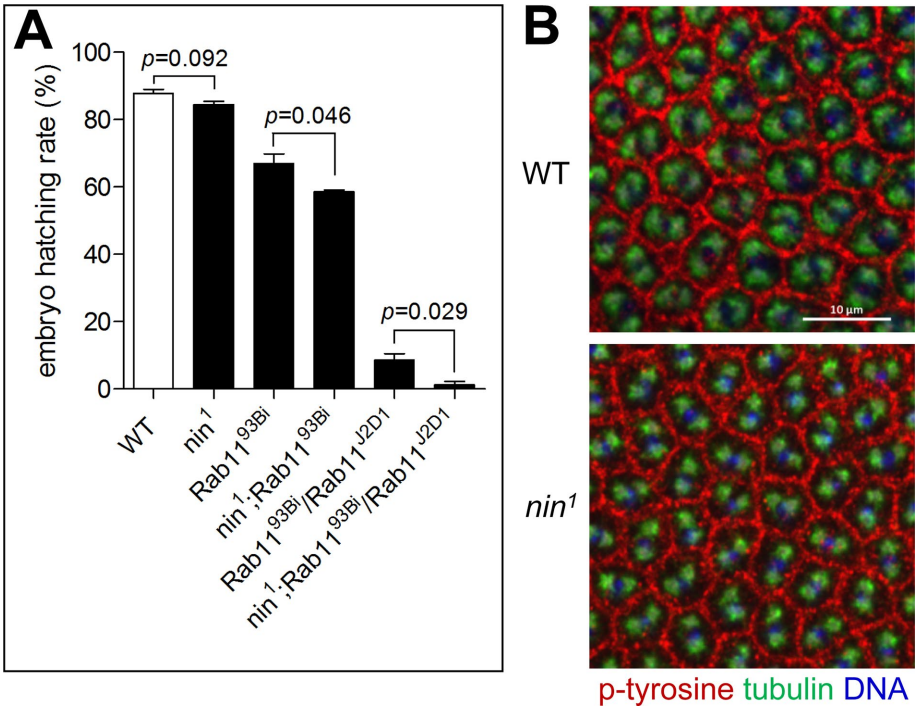

FIGURE 8: Nin is not essential for embryo development and *nin*^{1} appears to not interact genetically with *Rab11*. (A) *nin*^{1} embryos hatched at a slightly decreased rate (84.5 ± 1.0%) compared with wild type (87.8 ± 1.1%). Homozygous *Rab11*^{93Bi} showed a significantly reduced hatching rate of 66.9 ± 2.9% compared with wild-type, while addition of *nin*^{1} decreased the hatching rate further to 58.5 ± 0.5%. Only 8.5 ± 2.0% of transheterozygous *Rab11*^{93Bi}/*Rab11*^{J2D1} hatched. However, in combination with *nin*^{1} the hatch rate was reduced to 1.2 ± 1.0%. Three independent experiments were performed. 1000 embryos each were assayed for wild type and *nin*^{1}, and 750 embryos were assayed for each of the remaining genotypes. Error bars indicate SEM. (B) Representative images showing normal cleavage furrow formation in *nin*^{1} embryos. Embryos were stained with anti-α-tubulin (green), phospho-tyrosine (red, marker for cleavage furrow), and DAPI (blue).

Generation of *nin*^{1} deletion allele

A collection of ~300 potential *nin* deletion alleles was generated by mobilizing a P element transposon located within the 5′ UTR of the *nin* gene in the *Bsg25D*^{G13518} allele (Figure 6A) by crossing it through the germline of females carrying P transposase (CyO, PΔ2-3; BL#6394). All potential alleles were balanced with CyO, P(GAL4-Kr)^{DC3}, and P(UAS-GFP)^{DC7} (BL#5194). We isolated both *w*– and *w*$^{+}$ flies from these crosses. To screen for deletions in the *nin* gene caused by imprecise excision of the P element, adult flies or third-instar larvae homozygous or hemizygous over Df(2L)Exel6011 (BL#7497) were analyzed by PCR using primers indicated in Figure 6A and listed in Supplemental Table S1 using the single-fly PCR method (Gloor and Engels, 1992). Initial screening for deletion alleles was performed with primer pairs proximal to the transposon insertion site. Only one allele was found that lacked this sequence and failed to produce a PCR product; we named this allele *nin*^{1}. Subsequent PCR analysis was performed with primer pairs extending into the 3– end of *nin*, showing that *nin*^{1} has an ~3.5-kb deletion starting from the N-terminus and removing most of the coding sequence of all isoforms of the *nin* gene (Figure 6 and Supplemental Figure S4). Therefore *nin*^{1} is likely a null allele. The exact 3′ breakpoint of the deletion was not mapped at the nucleotide level but to within a 300–base pair region. A remnant of the original transposon remains at the 5′ end of the *nin*^{1} allele and retains the *w* minigene. Thus *nin*^{1} is tightly linked with a *white* minigene and has an orange eye color.

The *nin*^{1} allele was backcrossed with *w*^{1118} for six generations to remove other potential lesions on the chromosome and isogenize it with the control *w*^{1118} stock. The resulting *nin*^{1} deletion mutant could be maintained as a homozygous stock.

Antibodies

The following antibodies were used: mouse anti–α-tubulin (DM1A; 1:1000 for indirect immunofluorescence staining [IF], 1:10,000 for immunoblotting [IB]; Sigma-Aldrich, St. Louis, MO), rat monoclonal anti–α-tubulin (YL1/2; 1:1000 for IF; Thermo Fisher, Waltham, MA), mouse monoclonal anti-myc (9B11; 1:2000 for IF, 1:20,000 for IB; Cell Signaling Technology, Danvers, MA), rabbit or guinea pig anti-Cnn (1:1000 for IF; Zhang and Megraw, 2007), guinea pig anti–Nin N-terminus (1:100 for IF, 1:1000 for IB; Iampietro *et al.*, 2014), rabbit anti–Nin C-terminus (see later discussion; 1:2000 for IB), rat anti-Mira (1:100 for IF; a gift from Chris Doe, Institute of Molecular Biology, University of Oregon, Eugene, OR), rabbit anti-aPKC (C-20; 1:100 for IF; Santa Cruz Biotechnology, Dallas, TX), rabbit anti–phospho-histone H3 (1:1000 for IF; Upstate EMD Millipore, Darmstadt, Germany), mouse anti-phosphotyrosine (1:500 for IF; Santa Cruz Biotechnology), rabbit anti-Nuf (1:500 for IF; Rothwell *et al.*, 1998), anti–γ-tubulin (1:500 for IF; GTU-88; Sigma-Aldrich), anti-GM130

Expression pattern	Cross	F1 Phenotype
Throughout nervous system	Elav-GAL4 × UAS-Nin-GFP	Healthy and fertile
Neuroblast-specific	Worniu-GAL4 × UAS-Nin-GFP	Healthy and fertile
Global	Tub-GAL4/TM6B × UAS-Nin-GFP	Early pupal lethal
	Tub-GAL4/TM6B × UAS-GFP-Cnn	Healthy and fertile
	Tub-GAL4/TM6B × UAS-Bld10-GFP	Healthy and fertile
	Tub-GAL4/TM6B × UAS-Sas6-GFP	Healthy and fertile
	Tub-GAL4/TM6B × UAS-Rab11-YFP	Healthy and fertile

TABLE 1: Global Nin overexpression is lethal.

(1:1000 for IF; Abcam, Cambridge, United Kingdom), and guinea pig anti-Asterless (1:1000 for IF; a gift from Nasser Rusan, Cell Biology and Physiology Center, National Institutes of Health, Bethesda, MD). Anti-Dlg antibodies (1:100 for IF) were obtained from the Developmental Studies Hybridoma Bank, University of Iowa.

Generation of rabbit anti-Nin C-terminus antibodies

Sequences corresponding to amino acids 829–1026 of Nin-PB were cloned into pDEST-17 (Invitrogen) for expression of a 6×His-tagged protein in *E. coli* strain BL21(DE3)pLysE. Nin protein was isolated from *E. coli* in inclusion bodies, dissolved in 6M guanidine hydrochloride, centrifuged at 12,000 × *g* for 20 min, and purified by immobilized metal affinity chromatography with Ni^{2+}-charged Chelating Sepharose Fast Flow (GE Healthcare, Little Chalfont, United Kingdom). Purified protein was dialyzed against phosphate-buffered saline (PBS), and 3 mg purified by preparative minigel using 10% SDS–PAGE. The protein band was excised from the gel, and antibodies were raised in rabbits by Cocalico Biologicals. This antibody was used for Western blotting. A second antibody, used for immunostaining, was generated by immunizing rabbits (Covance, Princeton, NJ) with a synthetic peptide corresponding to amino acids 1074–1091 of Nin-PB. Antibodies were affinity-purified by peptide affinity chromatography using sulfolink resin (Pierce, Thermo Fisher).

Western blotting

6 h or overnight embryos were lysed in 2×SDS–PAGE loading buffer (100 mM Tris-HCl, pH 6.8, 4% SDS, 0.02% bromophenol blue, 20% glycerol, 5% β-mercaptoethanol). Third instar wandering larval brains (n = 10) were dissected and lysed in 20 µl of 2×SDS–PAGE loading buffer. Boiled embryo and larval brain lysates were resolved by 7.5% SDS–PAGE and then transferred to nitrocellulose membranes (Santa Cruz) using a semidry transfer system (Bio-Rad, Hercules, CA). After blocking with 5% nonfat milk in 1×TBS for 1 h at room temperature, membranes were probed with primary antibodies diluted in 1×TBS containing 0.1% Tween and 2.5% nonfat milk overnight at 4°C. The membrane was then washed with 1×TBS containing 0.1% Tween three times for 5 min each. The washed membrane was incubated with secondary antibodies conjugated with IRDye-800CW or IRDye-680LT (1:20,000) for 1 h at room temperature. Signal was detected with an Odyssey Infrared Imaging system (LI-COR Bioscience, Lincoln, NE), followed by image processing in Adobe Photoshop CS4.

Immunostaining of *Drosophila* tissues

Nin imaging was performed using anti-Nin antibodies (either the N-term guinea pig one or one of the C-terminal rabbit ones; see above), unless otherwise indicated on the figures and in the figure legends. Larval brain neuroblast staining was performed as previously described (Kao and Megraw, 2009). Briefly, brains from third instar wandering larvae were dissected in PEM (100 mM PIPES, pH 6.9, 1 mM EGTA, and 2 mM $MgSO_4$) and transferred to a 4 µl drop of PEM on a clean slide, which was subsequently covered with a 22 × 22 mm siliconized coverslip containing 1 µl of 18.5% formaldehyde in PEM, allowing the weight of the coverslip to flatten the larval brains (two per slide) for 30 s. The slide was then immersed in liquid nitrogen for snap freezing. The coverslip was flipped off using a razor blade, and the glass slide with the brain attached was immediately fixed in −20°C methanol for 10 min, followed by a rinse in PBS. A hydrophobic ring is drawn around the brain tissue using a Super Pap Pen (Immunotech, Monrovia, CA), and 50 µl of primary or secondary antibodies solution (diluted in PBS containing 5% bovine serum albumin (BSA) and 0.1% saponin) was pipetted over the brain and contained within the ring. The slides were incubated in a humid chamber at room temperature for 1–2 h.

To examine polarity protein localization in larval brain neuroblasts and to assess neuroblast number and spindle orientation in whole larval brains, whole-mount larval brain staining was performed as previously described (Singh *et al.*, 2014). Third instar wandering larval brains were dissected in PBS and fixed for 20 min in 4% paraformaldehyde in PBS. The fixed larval brains were washed twice with PBS, followed by blocking with PBSBT (1×PBS, 0.1% Triton X-100, and 1% BSA) for 1 h and incubated with primary and secondary antibodies in PBSBT.

Embryo collecting, fixation, and staining were performed as previously described (Megraw *et al.*, 1999). Fixed embryos were blocked 1 h with PBSBT and incubated with primary and secondary antibodies in PBSBT. Fixed and stained embryos were equilibrated in 80% glycerol in PBS, and were mounted in 25 µl of this mounting medium and stored at 4°C.

Whole-mount wing disk staining was similar to the larval brain staining as above described. Larval muscle was fixed and stained as described (Januschke *et al.*, 2006). Briefly, third instar larvae were fileted and gutted, then the carcasses were extracted with 0.5% Triton X-100 prior to fixation in ice-cold methanol for 20 min. Following rehydration, muscle filets were blocked for 1 h with PBSBT and incubated with primary and secondary antibodies in PBSBT. Fixed and stained filets were equilibrated in 80% glycerol in PBS, and were mounted in this mounting medium and stored at 4°C.

Samples were imaged using a Nikon A1 laser scanning confocal microscope (Nikon, Japan) using a 60×/1.49NA oil immersion objective, or on a Leica SP5 laser scanning confocal microscope using a 40×/1.4NA or a 63×/1.4NA oil immersion objective. Images were captured with a spacing of 0.5 µm between z-sections. All images are maximum intensity projections of z stacks, processed using the Nikon NIS-Elements software or the Leica SP5 software and Adobe Photoshop CS5.

Identification of daughter and mother centrosome in neuroblasts

In fixed samples, neuroblasts were generally identified as Mira-positive cells, or cells with >10 µm in diameter. The volume and fluorescence intensity of Cnn at centrosomes was used to distinguish mother and daughter centrosomes: the centrosome with larger diameter and higher fluorescence intensity were defined as the daughter centrosome (Rusan and Peifer, 2007; Januschke *et al.*, 2011; Januschke *et al.*, 2013). In telophase neuroblasts, we could readily distinguish daughter from mother centrosome because the daughter centrosome segregates with the neuroblast, which has a larger size relative to the ganglion mother cell, where the mother centrosome segregates.

Analysis of mitotic spindle orientation and measurement of neuroblast number in larval brain

To assess mitotic spindle orientation of neuroblasts in fixed larval brains, we plotted the angle between the mitotic spindle axis using tubulin staining or Cnn staining, with a tangential line of Mira crescent using Image J (NIH). For measurement of brain neuroblasts in wandering stage larvae, we didn't include either the type II neuroblasts in the dorsoposterior brain that have more complex lineages or the optic lobe neuroblasts (Cabernard and Doe, 2009). The Mira positive neuroblasts were counted. The counts from the central

brain region and from the whole brain were quantified in Figure 7 and Supplemental Figure S6, respectively. The number of neuroblasts is shown as mean ± SEM from eight larval brains.

Locomotor ability analysis of adult fly

Fly locomotor performance assays were performed as previously described (Ali *et al.*, 2011). Briefly, 10 well-fed male flies aged 6–8 d were placed into an empty chamber consisting of two conjoined plastic vials. Flies were gently tapped down to the bottom of vial and then given 10 s to climb a vertical 8 cm distance on the vial. The number of flies that successfully climbed 8 cm distance was recorded. The same set of flies were tested following a 1 min rest: this was repeated five times. The climbing index was calculated by the percent of flies passing the 8 cm mark and calculated as the mean ± SEM from at least five independent sets of 10 flies for each genotype.

Analysis of embryo hatch rate

nin^{1} mutant embryos were collected from *nin*^{1} homozygous females after crossing *nin*^{1} homozygous males and females. Rab11-deficient embryos were collected either from homozygous females bearing the hypomorphic allele *Rab11*^{93Bi} or from transheterozygous females bearing a combination of the amorphic *Rab11*^{J2D1} and hypomorphic *Rab11*^{93Bi} alleles (Jankovics *et al.*, 2001). Double mutants bearing a combination of *nin*^{1} and *Rab11*^{93Bi} alleles, or a combination of *nin*^{1} and *Rab11*^{93Bi}/*Rab11*^{J2D1} alleles were also tested.

Embryo hatching rate was determined with a method modified from (Kao and Megraw, 2009). Briefly, to count the hatching rate of embryos, 250 embryos for each genotype were lined up on apple juice/agar plates. After 2 d of incubation at 25°C, hatched and unhatched embryos were counted. Data shown were from at least three independent assays with a total number of at least 750 embryos from each genotype. Student's *t*-test was used to analyze the significance, and hatching differences were considered statistically significant when $p < 0.05$.

ACKNOWLEDGMENTS

We thank Ling-Rong Kao for help with the *nin* mutant screen. We thank Eric Lecuyer, Chris Doe, and Nasser Rusan for antibodies, Neema Salimi for providing the Pearl script to analyze microtubule emergence points, and the Vale lab at the University of California, San Francisco, for access to the spinning-disk confocal microscope for live-cell imaging experiments. We thank Neema Salimi for help with image analysis and David Gorczyca and Frozan Safi for *Drosophila* muscle preparations. We thank the Bloomington *Drosophila* Stock Center for fly stocks and Batory Foods for their generous donation of fly food reagents to support this research. This work was supported by a grant to Y.Z. from the Bryan W. Robinson Foundation and by National Institutes of Health Grants GM068758 and GM119078 to T.L.M.

REFERENCES

Al-Dosari MS, Shaheen R, Colak D, Alkuraya FS (2010). Novel CENPJ mutation causes Seckel syndrome. J Med Genet 47, 411–414.

Ali YO, Escala W, Ruan K, Zhai RG (2011). Assaying locomotor, learning, and memory deficits in Drosophila models of neurodegeneration. J Vis Exp 2011, 492504.

Antonczak AK, Mullee LI, Wang Y, Comartin D, Inoue T, Pelletier L, Morrison CG (2016). Opposing effects of pericentrin and microcephalin on the pericentriolar material regulate CHK1 activation in the DNA damage response. Oncogene 35, 2003–2010.

Arquint C, Gabryjonczyk AM, Nigg EA (2014). Centrosomes as signalling centres. Philos Trans R Soc Lond B Biol Sci 369, 20130464.

Banga SS, Shenkar R, Boyd JB (1986). Hypersensitivity of Drosophila mei-41 mutants to hydroxyurea is associated with reduced mitotic chromosome stability. Mutat Res 163, 157–165.

Basto R, Lau J, Vinogradova T, Gardiol A, Woods CG, Khodjakov A, Raff JW (2006). Flies without centrioles. Cell 125, 1375–1386.

Boyer PD, Mahoney PA, Lengyel JA (1987). Molecular characterization of bsg25D: a blastoderm-specific locus of Drosophila melanogaster. Nucleic Acids Res 15, 2309–2325.

Bugnard E, Zaal KJ, Ralston E (2005). Reorganization of microtubule nucleation during muscle differentiation. Cell Motil Cytoskeleton 60, 1–13.

Cabernard C, Doe CQ (2009). Apical/basal spindle orientation is required for neuroblast homeostasis and neuronal differentiation in Drosophila. Dev Cell 17, 134–141.

Caldwell JC, Miller MM, Wing S, Soll DR, Eberl DF (2003). Dynamic analysis of larval locomotion in Drosophila chordotonal organ mutants. Proc Natl Acad Sci USA 100, 16053–16058.

Carvalho-Santos Z, Machado P, Alvarez-Martins I, Gouveia SM, Jana SC, Duarte P, Amado T, Branco P, Freitas MC, Silva ST, *et al.* (2012). BLD10/CEP135 is a microtubule-associated protein that controls the formation of the flagellum central microtubule pair. Dev Cell 23, 412–424.

Casenghi M, Barr FA, Nigg EA (2005). Phosphorylation of Nlp by Plk1 negatively regulates its dynein-dynactin-dependent targeting to the centrosome. J Cell Sci 118, 5101–5108.

Casenghi M, Meraldi P, Weinhart U, Duncan PI, Korner R, Nigg EA (2003). Polo-like kinase 1 regulates Nlp, a centrosome protein involved in microtubule nucleation. Dev Cell 5, 113–125.

Chavali PL, Peset I, Gergely F (2015). Centrosomes and mitotic spindle poles: a recent liaison? Biochem Soc Trans 43, 13–18.

Chavali PL, Putz M, Gergely F (2014). Small organelle, big responsibility: the role of centrosomes in development and disease. Philos Trans R Soc Lond B Biol Sci 369, 20130468.

Chen JV, Megraw TL (2014). Spermitin: a novel mitochondrial protein in Drosophila spermatids. PLoS One 9, e108802.

Conduit PT, Raff JW (2010). Cnn dynamics drive centrosome size asymmetry to ensure daughter centriole retention in Drosophila neuroblasts. Curr Biol 20, 2187–2192.

Dauber A, Lafranchi SH, Maliga Z, Lui JC, Moon JE, McDeed C, Henke K, Zonana J, Kingman GA, Pers TH, *et al.* (2012). Novel microcephalic primordial dwarfism disorder associated with variants in the centrosomal protein ninein. J Clin Endocrinol Metab 97, E2140–E2151.

Debec A, Sullivan W, Bettencourt-Dias M (2010). Centrioles: active players or passengers during mitosis? Cell Mol Life Sci 67, 2173–2194.

Delgehyr N, Sillibourne J, Bornens M (2005). Microtubule nucleation and anchoring at the centrosome are independent processes linked by ninein function. J Cell Sci 118, 1565–1575.

de Saint Phalle B, Sullivan W (1998). Spindle assembly and mitosis without centrosomes in parthenogenetic Sciara embryos. J Cell Biol 141, 1383–1391.

Eberl DF, Hardy RW, Kernan MJ (2000). Genetically similar transduction mechanisms for touch and hearing in Drosophila. J Neurosci 20, 5981–5988.

Giansanti MG, Gatti M, Bonaccorsi S (2001). The role of centrosomes and astral microtubules during asymmetric division of Drosophila neuroblasts. Development 128, 1137–1145.

Gloor G, Engels W (1992). Single-fly DNA preps for PCR. Drosophila Information Service 71, 148–149.

Goodwin SS, Vale RD (2010). Patronin regulates the microtubule network by protecting microtubule minus ends. Cell 143, 263–274.

Gopalakrishnan J, Mennella V, Blachon S, Zhai B, Smith AH, Megraw TL, Nicastro D, Gygi SP, Agard DA, Avidor-Reiss T (2011). Sas-4 provides a scaffold for cytoplasmic complexes and tethers them in a centrosome. Nat Commun 2, 359.

Graser S, Stierhof YD, Lavoie SB, Gassner OS, Lamla S, Le Clech M, Nigg EA (2007). Cep164, a novel centriole appendage protein required for primary cilium formation. J Cell Biol 179, 321–330.

Guruharsha KG, Rual JF, Zhai B, Mintseris J, Vaidya P, Vaidya N, Beekman C, Wong C, Rhee DY, Cenaj O, *et al.* (2011). A protein complex network of Drosophila melanogaster. Cell 147, 690–703.

Iampietro C, Bergalet J, Wang X, Cody NA, Chin A, Lefebvre FA, Douziech M, Krause HM, Lecuyer E (2014). Developmentally regulated elimination of damaged nuclei involves a Chk2-dependent mechanism of mRNA nuclear retention. Dev Cell 29, 468–481.

Jankovics F, Sinka R, Erdelyi M (2001). An interaction type of genetic screen reveals a role of the Rab11 gene in oskar mRNA localization in the developing Drosophila melanogaster oocyte. Genetics 158, 1177–1188.

Januschke J, Gervais L, Gillet L, Keryer G, Bornens M, Guichet A (2006). The centrosome-nucleus complex and microtubule organization in the Drosophila oocyte. Development 133, 129–139.
Januschke J, Llamazares S, Reina J, Gonzalez C (2011). Drosophila neuroblasts retain the daughter centrosome. Nat Commun 2, 243.
Januschke J, Reina J, Llamazares S, Bertran T, Rossi F, Roig J, Gonzalez C (2013). Centrobin controls mother-daughter centriole asymmetry in Drosophila neuroblasts. Nat Cell Biol 15, 241–248.
Kalay E, Yigit G, Aslan Y, Brown KE, Pohl E, Bicknell LS, Kayserili H, Li Y, Tuysuz B, Nurnberg G, *et al.* (2011). CEP152 is a genome maintenance protein disrupted in Seckel syndrome. Nat Genet 43, 23–26.
Kao LR, Megraw TL (2004). RNAi in cultured Drosophila cells. Methods Mol Biol 247, 443–457.
Kao LR, Megraw TL (2009). Centrocortin cooperates with centrosomin to organize Drosophila embryonic cleavage furrows. Curr Biol 19, 937–942.
Karr TL, Alberts BM (1986). Organization of the cytoskeleton in early Drosophila embryos. J Cell Biol 102, 1494–1509.
Khodjakov A, Cole RW, Oakley BR, Rieder CL (2000). Centrosome-independent mitotic spindle formation in vertebrates. Curr Biol 10, 59–67.
Klingseisen A, Jackson AP (2011). Mechanisms and pathways of growth failure in primordial dwarfism. Genes Dev 25, 2011–2024.
Lecland N, Debec A, Delmas A, Moutinho-Pereira S, Malmanche N, Bouissou A, Dupre C, Jourdan A, Raynaud-Messina B, Maiato H, *et al.* (2013). Establishment and mitotic characterization of new Drosophila acentriolar cell lines from DSas-4 mutant. Biol Open 2, 314–323.
Li K, Xu EY, Cecil JK, Turner FR, Megraw TL, Kaufman TC (1998). Drosophila centrosomin protein is required for male meiosis and assembly of the flagellar axoneme. J Cell Biol 141, 455–467.
Majewski F, Goecke T (1982). Studies of microcephalic primordial dwarfism I: approach to a delineation of the Seckel syndrome. Am J Med Genet 12, 7–21.
Matis M, Russler-Germain DA, Hu Q, Tomlin CJ, Axelrod JD (2014). Microtubules provide directional information for core PCP function. Elife 3, e02893.
Megraw TL, Kao LR, Kaufman TC (2001). Zygotic development without functional mitotic centrosomes. Curr Biol 11, 116–120.
Megraw TL, Li K, Kao LR, Kaufman TC (1999). The centrosomin protein is required for centrosome assembly and function during cleavage in Drosophila. Development 126, 2829–2839.
Megraw TL, Sharkey JT, Nowakowski RS (2011). Cdk5rap2 exposes the centrosomal root of microcephaly syndromes. Trends Cell Biol 21, 470–480.
Mennella V, Agard DA, Huang B, Pelletier L (2014). Amorphous no more: subdiffraction view of the pericentriolar material architecture. Trends Cell Biol 24, 188–197.
Mennella V, Keszthelyi B, McDonald KL, Chhun B, Kan F, Rogers GC, Huang B, Agard DA (2012). Subdiffraction-resolution fluorescence microscopy reveals a domain of the centrosome critical for pericentriolar material organization. Nat Cell Biol 14, 1159–1168.
Mennella V, Rogers GC, Rogers SL, Buster DW, Vale RD, Sharp DJ (2005). Functionally distinct kinesin-13 family members cooperate to regulate microtubule dynamics during interphase. Nat Cell Biol 7, 235–245.
Mogensen MM, Malik A, Piel M, Bouckson-Castaing V, Bornens M (2000). Microtubule minus-end anchorage at centrosomal and non-centrosomal sites: the role of ninein. J Cell Sci 113, 3013–3023.
Mogensen MM, Tucker JB, Stebbings H (1989). Microtubule polarities indicate that nucleation and capture of microtubules occurs at cell surfaces in Drosophila. J Cell Biol 108, 1445–1452.
Mottier-Pavie V, Megraw TL (2009). Drosophila bld10 is a centriolar protein that regulates centriole, basal body, and motile cilium assembly. Mol Biol Cell 20, 2605–2614.
O'Driscoll M, Ruiz-Perez VL, Woods CG, Jeggo PA, Goodship JA (2003). A splicing mutation affecting expression of ataxia-telangiectasia and Rad3-related protein (ATR) results in Seckel syndrome. Nat Genet 33, 497–501.
Ogi T, Walker S, Stiff T, Hobson E, Limsirichaikul S, Carpenter G, Prescott K, Suri M, Byrd PJ, Matsuse M, *et al.* (2012). Identification of the first ATRIP-deficient patient and novel mutations in ATR define a clinical spectrum for ATR-ATRIP Seckel Syndrome. PLoS Genet 8, e1002945.
Ou YY, Mack GJ, Zhang M, Rattner JB (2002). CEP110 and ninein are located in a specific domain of the centrosome associated with centrosome maturation. J Cell Sci 115, 1825–1835.
Peel N, Stevens NR, Basto R, Raff JW (2007). Overexpressing centriole-replication proteins in vivo induces centriole overduplication and de novo formation. Curr Biol 17, 834–843.
Qvist P, Huertas P, Jimeno S, Nyegaard M, Hassan MJ, Jackson SP, Borglum AD (2011). CtIP mutations cause Seckel and Jawad syndromes. PLoS Genet 7, e1002310.
Riggs B, Rothwell W, Mische S, Hickson GR, Matheson J, Hays TS, Gould GW, Sullivan W (2003). Actin cytoskeleton remodeling during early Drosophila furrow formation requires recycling endosomal components Nuclear-fallout and Rab11. J Cell Biol 163, 143–154.
Rogers GC, Rusan NM, Peifer M, Rogers SL (2008). A multicomponent assembly pathway contributes to the formation of acentrosomal microtubule arrays in interphase Drosophila cells. Mol Biol Cell 19, 3163–3178.
Rogers SL, Rogers GC, Sharp DJ, Vale RD (2002). Drosophila EB1 is important for proper assembly, dynamics, and positioning of the mitotic spindle. J Cell Biol 158, 873–884.
Roque H, Wainman A, Richens J, Kozyrska K, Franz A, Raff JW (2012). Drosophila Cep135/Bld10 maintains proper centriole structure but is dispensable for cartwheel formation. J Cell Sci 125, 5881–5886.
Rothwell WF, Fogarty P, Field CM, Sullivan W (1998). Nuclear-fallout, a Drosophila protein that cycles from the cytoplasm to the centrosomes, regulates cortical microfilament organization. Development 125, 1295–1303.
Rusan NM, Peifer M (2007). A role for a novel centrosome cycle in asymmetric cell division. J Cell Biol 177, 13–20.
Salzmann V, Chen C, Chiang CY, Tiyaboonchai A, Mayer M, Yamashita YM (2014). Centrosome-dependent asymmetric inheritance of the midbody ring in Drosophila germline stem cell division. Mol Biol Cell 25, 267–275.
Shaheen R, Faqeih E, Ansari S, Abdel-Salam G, Al-Hassnan ZN, Al-Shidi T, Alomar R, Sogaty S, Alkuraya FS (2014). Genomic analysis of primordial dwarfism reveals novel disease genes. Genome Res 24, 291–299.
Singh P, Ramdas Nair A, Cabernard C (2014). The centriolar protein Bld10/Cep135 is required to establish centrosome asymmetry in Drosophila neuroblasts. Curr Biol 24, 1548–1555.
Sir JH, Barr AR, Nicholas AK, Carvalho OP, Khurshid M, Sossick A, Reichelt S, D'Santos C, Woods CG, Gergely F (2011). A primary microcephaly protein complex forms a ring around parental centrioles. Nat Genet 43, 1147–1153.
Tassin AM, Paintrand M, Berger EG, Bornens M (1985). The Golgi apparatus remains associated with microtubule organizing centers during myogenesis. J Cell Biol 101, 630–638.
Vaizel-Ohayon D, Schejter ED (1999). Mutations in centrosomin reveal requirements for centrosomal function during early Drosophila embryogenesis. Curr Biol 9, 889–898.
Wang S, Wu D, Quintin S, Green RA, Cheerambathur DK, Ochoa SD, Desai A, Oegema K (2015). NOCA-1 functions with gamma-tubulin and in parallel to Patronin to assemble non-centrosomal microtubule arrays in C. elegans. Elife 4.
Wang WJ, Soni RK, Uryu K, Tsou MF (2011). The conversion of centrioles to centrosomes: essential coupling of duplication with segregation. J Cell Biol 193, 727–739.
Wang X, Tsai JW, Imai JH, Lian WN, Vallee RB, Shi SH (2009). Asymmetric centrosome inheritance maintains neural progenitors in the neocortex. Nature 461, 947–955.
Woodruff JB, Wueseke O, Hyman AA (2014). Pericentriolar material structure and dynamics. Philos Trans R Soc Lond B Biol Sci 369, 20130459.
Yamashita YM, Mahowald AP, Perlin JR, Fuller MT (2007). Asymmetric inheritance of mother versus daughter centrosome in stem cell division. Science 315, 518–521.
Zhang J, Megraw TL (2007). Proper recruitment of gamma-tubulin and D-TACC/Msps to embryonic Drosophila centrosomes requires Centrosomin Motif 1. Mol Biol Cell 18, 4037–4049.